A theoretical study of the CH3+C2H2 reaction

Eric W. Diau, M. C. Lin, and C. F. Melius

Citation: J. Chem. Phys. **101**, 3923 (1994); doi: 10.1063/1.467510
View online: http://dx.doi.org/10.1063/1.467510
View Table of Contents: http://jcp.aip.org/resource/1/JCPSA6/v101/i5
Published by the American Institute of Physics.

A theoretical study of the $CH_3+C_2H_2$ reaction

Eric W. Diau and M. C. Lin[a)]
Department of Chemistry, Emory University, Atlanta, Georgia 30322

C. F. Melius
Combustion Research Facility, Sandia National Laboratories, Livermore, California 94550

(Received 15 February 1994; accepted 13 May 1994)

The rate constants for the formation of various products in the $CH_3+C_2H_2$ reaction have been computed by multichannel RRKM calculations using the molecular and transition-state parameters predicted by the BAC-MP4 method. The results of the calculations agree quantitatively with experimental data obtained under varying conditions: $T=300$–2200 K, $P=30$–2500 Torr. At low temperatures ($T<1300$ K), the $CH_3+C_2H_2$ reaction is dominated by the addition-stabilization process producing $CH_3C_2H_2$. Under high-temperature ($T>1400$ K) and atmospheric-pressure conditions, the reaction occurs primarily by the CH_3-for-H displacement process producing CH_3C_2H, a likely source of the C_3H_3 radical (which has recently been shown to be a key precursor of C_6H_6 in hydrocarbon combustion reactions).

I. INTRODUCTION

The recombination reaction of the propargyl radical, $C_3H_3+C_3H_3\rightarrow C_6H_6$, has recently been identified as a potential source of benzene,[1–3] an important building block of polyaromatic hydrocarbons (PAHs), which are likely precursors to soot in hydrocarbon combustion reactions. On account of the observation of a high concentration of the C_3H_3 radical, coexisting with an even higher concentration of CH_3 in a premixed, lightly sooting C_2H_2 flame,[4] the relationship between the C_3H_3 radical and the $CH_3+C_2H_2$ reaction becomes evident and theoretically interesting.

In principle, the $CH_3+C_2H_2$ reaction may take place via the following paths:

$$CH_3+C_2H_2 \underset{-a}{\overset{a}{\rightleftharpoons}} CH_3CH=CH^{\dagger} \overset{b}{\rightarrow} CH_3C_2H+H$$

$$\overset{c}{\rightarrow} CH_2-CH=CH_2$$

$$\overset{d}{\rightarrow} CH_3C_2H_2(+M),$$

where $CH_3CH=CH^{\dagger}$ is the chemically activated, excited adduct. Because of the relatively high stability of the adduct and the expected high barriers for steps (b) and (c) comparing with that for the addition step (a), the effect of pressure on the overall rate of the $CH_3+C_2H_2$ reaction may be quite prevalent. This pressure effect, which has not been carefully investigated previously, may be responsible in part for the large deviation in the reported rate constants measured at low temperatures (370–515 K),[5–7] at which the formation of $CH_3C_2H_2$ is a dominant process. Recently, Hidaka *et al.*[8] obtained the rate constant for step (b), the CH_3-for-H displacement reaction, over the temperature range 1400–2200 K; the rate constant differs considerably from that for the addition process as one would expect. These experimental data are summarized in Table I for comparison. Also included in the table are our kinetically modeled results, based on the experimental data of Garcia-Dominguez and Trotman-Dickenson,[6] using a more comprehensive set of reaction mechanism.[9]

In order to elucidate the effects of pressure and temperature on product formation via different channels as well as to reconcile the apparent large discrepancy among the values of rate constants obtained by different investigators with varying experimental techniques (see Table I), we have carried out detailed quantum-chemical calculations using the fourth-order Møller–Plesset perturbation method with bond-additivity corrections (BAC-MP4)[10–12] for reactants, transition states, and intermediates involved in the reaction. These theoretical data are used to calculate the rate constants for individual reaction channels by means of the RRKM theory[13] under varying T, P conditions.

II. RESULTS AND DISCUSSION

A. BAC-MP4 calculations

The BAC-MP4 technique employed in the present calculations of molecular structures, vibrational frequencies and heats of formation for various species involved in the $CH_3+C_2H_2$ reaction has been described in detail previously.[10–12] The accuracy of the technique for prediction of the heats of formation of ground-state molecules, including free radicals, has been discussed in several of the recent papers on the technique,[11,12,14,15] while its validity in predicting the rate constants for chemical reactions has been illustrated for a variety of processes involving H/C/N/O-containing species.[16–20]

A brief general overview of the technique is presented as follows: Equilibrium geometries and harmonic frequencies were computed at the HF/6-31G* level of theory, with restricted Hartree–Fock (RHF) theory for closed-shelled molecules and unrestricted Hartree–Fock (UHF) theory for the open-shelled molecules using the 6-31G* basis set. Vibrational frequencies calculated at this level of theory were systematically scaled down by a factor of 0.893. For the improvement in the computed energies, electronic correlation has been made by performing MP4 (SDTQ) calculations

a)Author to whom correspondence should be addressed.

 0021-9606/94/101(5)/3923/5/$6.00

TABLE I. Rate constants for the $CH_3+C_2H_2$ reaction reported by different investigators.

Investigator	P/Torr	T/K	A[a]	E/R[a]
Mendelcorn and Steacie[b]	26-59	417-514	1.7×10^{-13}	2770
Garcia-Domingues and Trotman-Dickenson[c]	28-89	371-479	4.2×10^{-13}	3880
			$(2.4\times10^{-13}$	3485)[d]
Holt and Kerr[e]	623-792	379-487	1.0×10^{-12}	3880
Landers and Volman[f]	60-286	403-437	--	2570
Hidaka *et al.*[g]	1750-2810	1400-2200	1.0×10^{-11}	8560

[a]The frequency factor, A, is given in units of cm^3/s and the activation energy in K.
[b]Reference 5.
[c]Reference 6.
[d]Reference 9; it should be mentioned that the experimental data of Mendelcorn and Steacie (Ref. 5) were of poor quality and insufficient for kinetic modeling.
[e]Reference 7.
[f]Measured by the rate of pressure change [J. Am. Chem. Soc. **79**, 2996 (1957)].
[g]Reference 8.

(fourth-order Møller–Plesset perturbation with single, double, triple, and quadruple substitutions), single-point calculations employing a 6-31G** (double-ζ plus polarization) basis set with the HF/g-31G* geometries. The electronic structure calculations were carried out with GAUSSIAN90 programs.[21]

The computed heats of formation presented in Table II have been empirically corrected by bond-additivity approximation for the systematic errors in the *ab initio* calculations, resulting mainly from basis-set truncation. The corrections depend principally on the bond type and bond distance with modifications for neighboring bonds. Additional corrections for electron spins, either to remove the effects of spin contamination for open-shell, unrestricted Hartree–Fock (UHF) calculations or to account for the UHF instability of closed-shell molecules. The sum of the BACs is combined with the MP4 (SDTQ) electronic energy and the zero-point energy (ZPE) to give a heat of formation at 0 K. Entropies, heat capacities, enthalpies, and free energies at higher temperatures were computed with statistical-mechanics equations.

The computed heats of formation, vibrational frequencies, and moments of inertia of reactants, intermediates, transition states, and products are summarized in Table II. Also given in the table are estimated errors for the heats of formation, stemming from the size of the BAC spin corrections and the consistency of the BAC-MP4 method with other levels of theory. There are greater uncertainties associated with the transition states because of the lack of convergence in the M–P perturbation theory energies. Additionally, the optimization of the geometry, obtained at the HF level of theory, may change the structure and energy within the uncertainties mentioned above when higher-level electron correlations are included.

B. Multichannel RRKM calculations

RRKM calculations have been carried out for the total and individual rate constants for all product channels of the $CH_3+C_2H_2$ reaction depicted by the mechanism presented in

TABLE II. Molecular and transition state parameters computed by the BAC-MP4 method for the $CH_3+C_2H_2$ reaction.[a]

Species or transition states	$\Delta H^0_{f,0}$[b] (kcal/mole)	I_a, I_b, I_c (amu)	ν_i (cm^{-1})	
CH_3	35.58±1.23	6.210	274.9	1375.0
		6.210	1375.0	2932.7
		12.421	3090.3	3090.3
C_2H_2	54.46±1.00	0	708.9	708.9
		49.699	788.0	788.0
		49.699	2006.2	3220.5
			3320.7	
CH_3CHCH(HCCH *cis*)	67.36±3.54	31.757	166.7	396.3
		189.374	573.5	799.7
		210.109	814.4	891.9
			1029.2	1094.1
			1210.3	1394.1
			1432.0	1453.7
			1481.4	2853.9
			2896.8	2909.2
			2935.1	3061.6
CH_3CHCH(HCCH *trans*)	67.70±3.54	37.672	160.8	381.0
		179.235	601.3	828.5
		205.880	860.1	874.9
			1020.5	1084.9
			1210.6	1390.1
			1426.6	1452.0
			1477.1	2854.1
			2899.5	2926.3
			2960.0	3050.7
CH_3CCH	47.62±2.60	11.117	350.8	350.8
		209.315	711.1	711.1
		209.315	880.1	1042.5
			1042.5	1042.5
			1451.2	1451.2
			2159.8	2870.5
			2931.5	2931.5
			3271.8	
CH_2CHCH_2	41.54±4.19	32.911	403.3	489.0
		175.302	511.4	696.7
		208.213	713.7	897.5
			924.2	960.0
			1117.2	1198.0
			1372.8	1462.3
			1471.1	2967.8
			2969.4	2979.0
			3052.2	3055.6
CH_3CCH_2	63.62±3.47	25.146	150.1	316.4
		207.489	472.6	837.0
		221.585	839.1	914.4
			1022.3	1094.4
			1360.4	1394.6
			1439.9	1452.4
			1512.0	2839.8
			2897.5	2911.7
			2916.3	3009.7
$CH_3+C_2H_2$ $\rightarrow CH_3CHCH$ (*cis*)	99.3±6.98	46.087	−503.6[c]	42.8[d]
		274.432	207.7	383.4
		308.422	413.6	467.0
			533.6	700.3
			711.7	831.8
			1392.5	1396.1

TABLE II. (*Continued.*)

Species or transition states	$\Delta H_{f,0}^0$[b] (kcal/mole)	I_a, I_b, I_c (amu)	ν_i (cm^{-1})	
			1519.9	2918.8
			3052.6	3062.2
			3168.6	3213.1
$CH_3CHCH(cis)$	104.53 ± 7.00	27.972	−836.9[c]	160.4
$\rightarrow CH_3CCH+H$		208.378	352.6	379.3
		225.285	462.6	551.2
			647.9	855.0
			1023.0	1041.0
			1395.5	1451.3
			1452.6	1788.8
			2873.9	2936.8
			2937.9	3233.6
$CH_3CHCH(cis)$	108.77 ± 5.00	46.382	−2373.5[c]	409.1
$\rightarrow CH_2CHCH_2$		144.179	597.3	649.3
		178.670	813.4	910.6
			914.3	994.0
			1017.5	1033.4
			1178.8	1365.1
			1421.5	1584.1
			2914.2	2989.5
			3007.0	3031.4

[a]The heats of formation, moments of inertia, and vibrational frequencies given for chemical reactions represent those of the transition states involved.
[b]Estimated uncertainties of heats of formation are included.
[c]Negative vibrational frequencies express those of the reaction coordinate involved.
[d]Using moments of inertia, $I=9.506$ amu instead of this value as a hindered internal rotor.

the preceding section. The energy diagram for the reaction system computed by the BAC-MP4 method is given in Fig. 1. On the basis of this comprehensive mechanism, the individual channel rate constants can be calculated by the following equations, previously derived for bimolecular reactions taking place via a long-lived intermediate:[22,23]

$$k_i(T)=\frac{1}{h}\frac{Q_{tr}^{\ddagger}}{Q_{CH_3}Q_{C_2H_2}}e^{-E_a^0/RT}\int_0^{\infty}\frac{k_i(E)f(E^{\ddagger})dE^{\ddagger}}{\Sigma k_i(E)+\omega}, \quad (1)$$

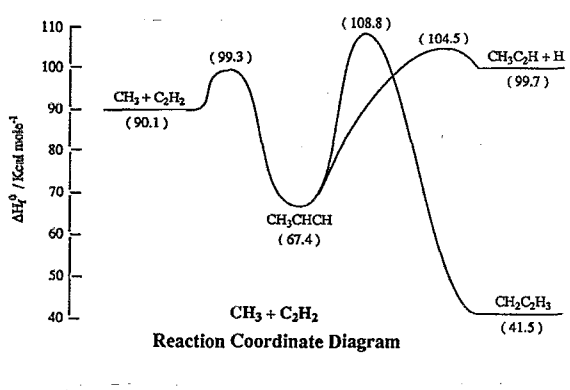

FIG. 1. Schematic energy diagram for the $CH_3+C_2H_2$ reaction based on the results of BAC-MP4 calculations.

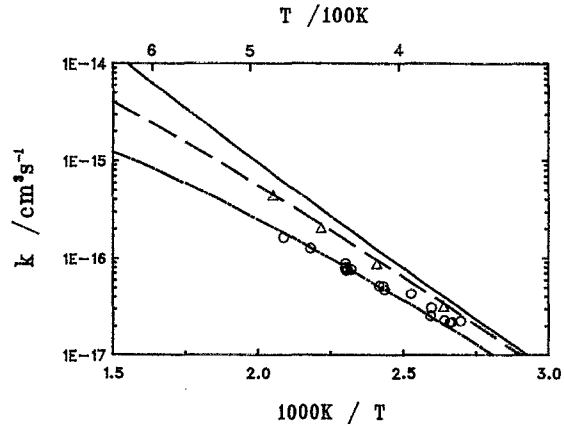

FIG. 2. Comparison of the calculated and experimental total rate constant for $CH_3+C_2H_2$ at low temperatures. Δ, experimental data of Holt and Kerr (Ref. 7) at 700 Torr pressure (mainly C_2H_2 and i-C_4H_{10}). ○, experimental data of Garcia-Dominguez and Trotman-Dickenson (Ref. 6) at 30–90 Torr pressure (mainly C_2H_2 and CH_3CHO), kinetically modeled with a detailed mechanism (Ref. 9). —, calculated k_t at $P=10^{14}$ Torr. – – –, calculated k_t at $P=700$ Torr. –·–, calculated k_t at $P=60$ Torr. All calculations were performed with $-\langle\Delta E\rangle=5$ kcal/mole and collision diameter of 5 Å.

$$k_d(T)=\frac{1}{h}\frac{Q_{tr}^{\ddagger}}{Q_{CH_3}Q_{C_2H_2}}e^{-E_a^0/RT}\int_0^{\infty}\frac{\omega f(E^{\ddagger})dE^{\ddagger}}{\Sigma k_i(E)+\omega}, \quad (2)$$

where $i=b$, c, and $(-a)$;

$$k_i(E)=C_i\sum P_i(E_i^{\ddagger})/hN(E), \quad (3)$$

$$f(E^{\ddagger})=\sum P_a(E_a^{\ddagger})\exp(-E_a^{\ddagger}/RT). \quad (4)$$

In the above equations, "‡" represents transition-state quantities. Q's are the total partition functions of the reactants, CH_3 and C_2H_2. $Q_{tr}^{\ddagger}$ represents the product of the translational and rotational partition function of the transition state associated with the addition process (a). $\Sigma P_i(E_i^{\ddagger})$ is the sum of states of the transition state for step (i) with energy $E_i^{\ddagger}$. $N(E)$ is the density of states of the chemically activated adduct, $CH_3CHCH^{\dagger}$, with total energy E. C_i is the product of statistical factor and the ratio of the overall rotational partition function of the transition state and the adduct for the unimolecular reaction step (i); $i=b$, c and $(-a)$. ω is the effective collision frequency for the deactivation of the excited adduct via step (d), calculated on the basis of Troe's weak collision treatment,[24] using an averaged step-size of 1 kcal/mole for Ar.

The total second-order rate constant measured experimentally for the disappearance of CH_3 radicals is given by

$$k_t(T)=\sum k_i(T), \quad (5)$$

with $i=b$, c and d, excluding $(-a)$, which regenerates CH_3. Both $k_b(T)$ and $k_c(T)$ can be calculated by Eq. (1), and $k_d(T)$ by Eq. (2). The results of the calculations using the molecular and transition state parameters summarized in Table II are compared in Figs. 2 and 3 with the experimental

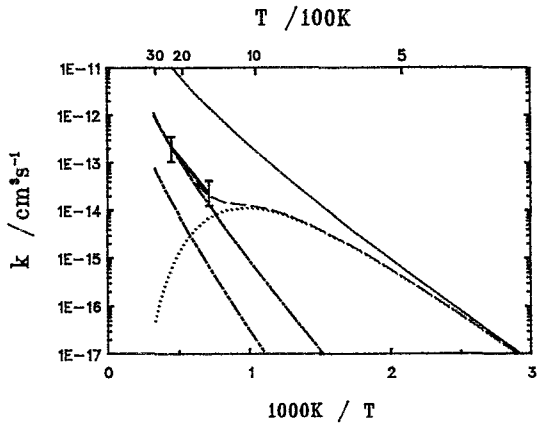

FIG. 3. Comparison of the calculated and experimental total rate constants for the total and individual product channels of the $CH_3+C_2H_2$ reaction at high temperatures. I, experimental data of Hidaka *et al.* (Ref. 8). —, calculated k_t at $P=10^{14}$ Torr Ar. - - -, calculated k_t at $P=3$ atm Ar. —·—, calculated k_b (CH_3C_2H+H) at 3 atm Ar. —··—, calculated k_c ($CH_2C_2H_3$) at 3 atm Ar. ···, calculated k_d ($CH_3C_2H_2$) at 3 atm Ar. All calculations were performed with $-\langle\Delta E\rangle=1$ kcal/mole and collision diameter of 4 Å.

data obtained under different T, P conditions.

In Fig. 2, the calculated values of k_t for the removal of CH_3 by C_2H_2 at 60 and 700 Torr total pressure are compared with the experimental data measured at the corresponding pressures by Garcia-Dominguez and Trotman-Dickenson,[6] and Hold and Kerr,[7] respectively. The agreement between the predicted total rate constants and the experimental data is quite good. The results of Garcia-Dominguez and Trotman-Dickenson[6] were measured randomly within the pressure range of 28–89 Torr at different temperatures. A detailed comparison of their data, with and without more refined modeling, is beyond the scope of this article; it will be presented separately elsewhere.[9]

In Fig. 3 we compare the calculated value of k_b for propyne production with that reported by Hidaka *et al.*[8] for the temperature range 1400–2200 K at pressures between 2.3 and 3.7 atm. The agreement between theory and experiment also appears to be very good. Under the conditions employed in the experiment, the $CH_3+C_2H_2$ reaction is dominated by the CH_3-for-H displacement process. Also presented in the figure are the calculated values for k_t^{∞}, the total rate constant at $P=10^{14}$ Torr, and k_c and k_d at 3 atm pressure. These results suggest that the second product channel producing the allyl radical (k_c) is relatively inconsequential below 3000 K, whereas the formation of the $CH_3C_2H_2$ adduct by collisional deactivation (k_d), although insignificant at higher temperatures, becomes prevalent at $T<1300$ K.

On account of the complexity of T, P effects, as revealed by the results presented in Figs. 2 and 3, we have also tabulated the values of k_b, k_c, and k_d in Table III for $P=10$, 100, 760, and 2280 Torr (Ar) at five temperatures between 300 and 2000 K. The results for the atmospheric pressure are fitted by least-squares to the following equations:

$$k_t=\begin{cases}1.30\times10^{5}\ T^{-5.50}e^{-6504/T}(300-1000\ \text{K})\\ 1.70\times10^{-41}\ T^{8.09}e^{+5078/T}(1000-3000\ \text{K})\end{cases}$$

$$k_b=3.18\times10^{-20}\ T^{2.42}e^{-6488/T}(300-3000\ \text{K})$$

$$k_c=2.32\times10^{-20}\ T^{2.21}e^{-8304/T}(300-3000\ \text{K})$$

$$k_d=\begin{cases}3.81\times10^{6}\ T^{-5.98}e^{-6709/T}(300-1000\ \text{K})\\ 6.40\times10^{32}\ T^{-13.67}e^{-14036/T}(1000-3000\ \text{K}),\end{cases}$$

all expressed in units of cm^3/s.

III. CONCLUSIONS

The rate constant for the $CH_3+C_2H_2$ reaction, a potential source of the C_3H_3 radical in hydrocarbon combustion processes, has been calculated over a wide range of conditions with the RRKM theory based on the thermochemical data computed by the BAC-MP4 technique. The calculated and experimental results agree closely across the entire temperature range studied experimentally (300–2200 K).

At low temperatures (300–500 K), the reaction was found to be dominated entirely by the pressure-dependent

TABLE III. Calculated rate constants for various product channels of $CH_3+C_2H_2$ with Ar as buffer gas.[a]

T / k_i / P	300			500			1000		
	b	c	d	b	c	d	b	c	d
10	1.59×10^{-23}	1.54×10^{-26}	3.45×10^{-19}	2.88×10^{-19}	2.55×10^{-21}	3.77×10^{-17}	8.51×10^{-16}	3.10×10^{-17}	1.25×10^{-16}
100	1.52×10^{-23}	1.53×10^{-26}	8.81×10^{-19}	2.85×10^{-19}	2.54×10^{-21}	1.70×10^{-16}	8.51×10^{-16}	3.10×10^{-17}	9.93×10^{-16}
760	1.16×10^{-23}	1.43×10^{-26}	1.26×10^{-18}	2.66×10^{-19}	2.49×10^{-21}	4.18×10^{-16}	8.48×10^{-16}	3.10×10^{-17}	1.97×10^{-14}
2280	7.87×10^{-24}	1.24×10^{-26}	1.36×10^{-18}	2.34×10^{-19}	2.37×10^{-21}	5.80×10^{-16}	8.43×10^{-16}	3.09×10^{-17}	1.12×10^{-14}
10^{14}	4.63×10^{-34}	1.68×10^{-36}	1.44×10^{-18}	6.74×10^{-29}	1.34×10^{-30}	9.46×10^{-16}	1.11×10^{-23}	5.61×10^{-25}	2.28×10^{-13}

	1500			2000		
	b	c	d	b	c	d
10	1.97×10^{-14}	1.10×10^{-15}	3.25×10^{-17}	1.20×10^{-13}	8.25×10^{-15}	5.96×10^{-18}
100	1.97×10^{-14}	1.10×10^{-15}	3.05×10^{-16}	1.20×10^{-13}	8.25×10^{-15}	5.89×10^{-17}
760	1.97×10^{-14}	1.10×10^{-15}	2.03×10^{-15}	1.20×10^{-13}	8.25×10^{-15}	4.31×10^{-16}
2280	1.96×10^{-14}	1.10×10^{-15}	5.43×10^{-15}	1.20×10^{-13}	8.25×10^{-15}	1.25×10^{-15}
10^{14}	3.45×10^{-21}	2.60×10^{-22}	2.07×10^{-12}	2.00×10^{-19}	1.57×10^{-20}	7.41×10^{-12}

[a]Rate constants are in units of cm^3/s; channels (b), (c), and (d) are described in the text; k_d at 10^{14} Torr ($p=\infty$) effectively represents k_a, the rate constant for the addition step, at all temperatures.

addition–stabilization process producing $CH_3C_2H_2$, a conclusion similarly reached earlier by Dean and Westmoreland using a QRRK model.[25] The strong pressure effect on the rate constants in this temperature regime, as revealed by the calculations, accounts in part for the existing large discrepancy between the experimental data obtained under different pressure conditions.[5–7]

At temperatures greater than 1400 K, the CH_3-for-H displacement process becomes dominant, while the formation of $CH_3C_2H_2$ by collisional deactivation diminishes rapidly with increasing temperature. The production of the $CH_2C_2H_3$ radical, which occurs via a tighter transition state with a greater energy barrier than the H-displacement process, is a relatively minor reaction even at temperatures as high as 3000 K, contrary to the estimate of Dean and Westmoreland.[25]

ACKNOWLEDGMENT

The authors gratefully acknowledge the Division of Basic Energy Science, Office of Energy Research, U.S. Department of Energy for the support of this work with Contract No. DE-FGO5-91ER14192 to Emory University.

[1] C. H. Wu and R. D. Kern, J. Phys. Chem. **91**, 6291 (1987).
[2] U. Alkemade and K. H. Homann, Z. Phys. Chem., N.F. **161**, 19 (1989).
[3] C. F. Melius, J. A. Miller and E. M. Elveth, in *The 24th Symposium (International) on Combustion* (The Combustion Institute, 1992), p. 621.
[4] P. R. Westmoreland, A. M. Dean, J. B. Howard, and J. P. Longwell, J. Phys. Chem. **93**, 8171 (1989).
[5] L. Mendelcorn and E. W. R. Steacie, Can. J. Chem. **32**, 474 (1954).
[6] J. A. Garcia-Dominguez and A.-F. Trotman-Dickenson, J. Chem. Soc. **940** (1962).
[7] P. M. Holt and J. A. Kerr, Int. J. Chem. Kinet. **9**, 185 (1977).
[8] Y. Hidaka, T. Nakamura, H. Tanaka, K. Inami, and H. Kawano, Int. J. Chem. Kinet. **22**, 701 (1990).
[9] E. W. Diau and M. C. Lin (to be published).
[10] C. F. Melius and J. S. Binkley, in *The 20th Symposium (International) on Combustion* (The Combustion Institute, Pittsburgh, PA, 1984), p. 575.
[11] C. F. Melius, in *Chemistry and Physics of Energetic Materials*, NATO SAI 309, edited by S. N. Bulusu (Kluwer Academic, The Netherlands, 1990), p. 21.
[12] P. Ho and C. F. Melius, J. Phys. Chem. **94**, 5120 (1990).
[13] W. Forst, *Theory of Unimolecular Reactions* (Academic, New York, 1973).
[14] M. D. Allendorf and C. F. Melius, J. Phys. Chem. **96**, 428 (1991).
[15] M. D. Allendorf and C. F. Melius, J. Phys. Chem. **97**, 720 (1993).
[16] N. S. Wang, D. L. Yang, M. C. Lin, and C. F. Melius, Int. J. Chem. Kinet. **23**, 151 (1991).
[17] K. H. Alridge, X. Liu, M. C. Lin, and C. F. Melius, Int. J. Chem. Kinet. **23**, 947 (1991).
[18] Y. He, X. Liu, M. C. Lin, and C. F. Melius, Int. J. Chem. Kinet. **23**, 1129 (1991).
[19] M. C. Lin, Y. He, and C. F. Melius, Int. J. Chem. Kinet. **24**, 489 (1992).
[20] D. L. Yang, T. Yu, M. C. Lin, and C. F. Melius, J. Chem. Phys. **97**, 222 (1992).
[21] M. J. Frisch, M. Head-Gordon, G. W. Trucks, J. B. Forssman, H. B. Schlegel, K. Raghavachari, M. Robb, J. S. Binkley, C. Gonzalez, D. J. Defrees, D. J. Fox, R. A. Whiteside, C. F. Melius, J. Baker, R. L. Martin, L. R. Kahn, J. J. P. Stewart, S. Topiol and J. A. Pople, GAUSSIAN 90, Revision F (Gaussian Inc., Pittsburgh, PA, 1990).
[22] D. S. Y. Hsu, W. M. Shaub, T. Creamer, D. Gutman, and M. C. Lin, Ber. Bunsenges. Phys. Chem. **87**, 909, 1983.
[23] M. R. Berman and M. C. Lin, J. Phys. Chem. **87**, 3933 (1983).
[24] J. Troe, J. Phys. Chem. **83**, 114 (1979).
[25] A. M. Dean and P. R. Westmoreland, Int. J. Chem. Kinet. **19**, 207 (1987).